

H-Mode Confinement in Tokamaks with Fully Metallic Walls: New Energy Confinement Scaling and Implications of the Reduced Size Dependence

G. Verdoolaege and J. Hall

Department of Applied Physics, Ghent University, Ghent, Belgium

20th European Fusion Theory Conference
Padua, Italy
October 3, 2023

1. Update of the global H-mode confinement database and scaling
2. Regression analysis for scaling laws
 - Conventional techniques
 - Geodesic least squares regression (GLS)
3. The ITPA20 confinement scaling law
4. Conclusions

1. Update of the global H-mode confinement database and scaling
2. Regression analysis for scaling laws
 - Conventional techniques
 - Geodesic least squares regression (GLS)
3. The ITPA20 confinement scaling law
4. Conclusions

Global confinement database update

- Motivation and use of scaling laws:
 - Based purely on experimental data (or almost)
 - Benchmark for experimental performance
 - Experimental design and modeling
- Multi-machine *Global H-mode Confinement Database* (*1989 → ITPA 2001)
- IPB98(y,2) ELMy H-mode global energy confinement scaling (1998)
- ITPA TC-28: Revision of ITER confinement database (2015–2020):
 - Add data closer to ITER conditions and expand parameter ranges
 - Add data from devices with fully metallic walls
 - Reconcile with single-machine scans (\bar{n}_e , $P_{l,th}$, β , ...)
 - Explore new predictor variables (e.g. δ , $n_{e,sep}$, torque, ...)
 - Robust regression analysis

Issues with IPB98

Density scaling Power degradation No δ scaling

$$\tau_{E,th} = 0.0562 I_p^{0.93} B_t^{0.15} \bar{n}_e^{0.41} P_{1,th}^{-0.69} R_{geo}^{1.97} (1+\delta)^{\alpha_\delta} \kappa_a^{0.78} \epsilon^{0.58} M_{eff}^{0.19}$$

β degradation No collisionality scaling No δ scaling

$$\Omega_i \tau_{E,th} = 4.24 \times 10^{-7} \rho_*^{-2.69} \beta_t^{-0.90} \nu_*^{-0.0081} q_{cyl}^{-2.99} (1+\delta)^{\alpha_\delta} \kappa_a^{3.29} \epsilon^{0.71} M_{eff}^{0.96}$$

Updates since DB4

- DB2.8 (IPB98) → DB3v13F → DB4.5 → *DB5.2.3*
- Enhanced data validation and W_{fast} in ASDEX Upgrade (AUG)
- New data:

Metallic wall *High-Z*

- AUG full W (AUG-W):
825 new points [1]
- JET ITER-like wall (ILW):
866 new points [2]

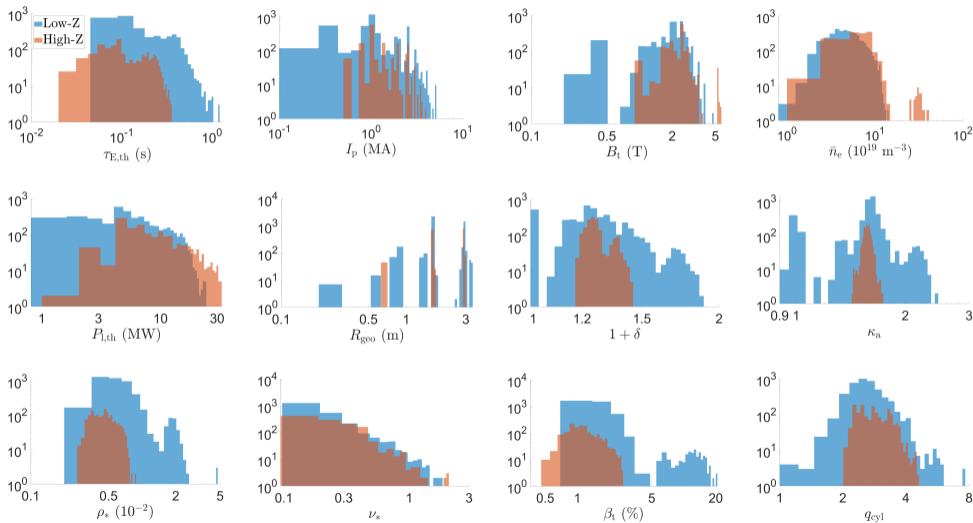
Carbon-based wall *Low-Z*

- AUG + JET: new data with high gas injection

[1] F. Ryter *et al.*, Nucl. Fusion, **61**, 046030, 2021

[2] M. Maslov *et al.*, Nucl. Fusion, **60**, 036007, 2020

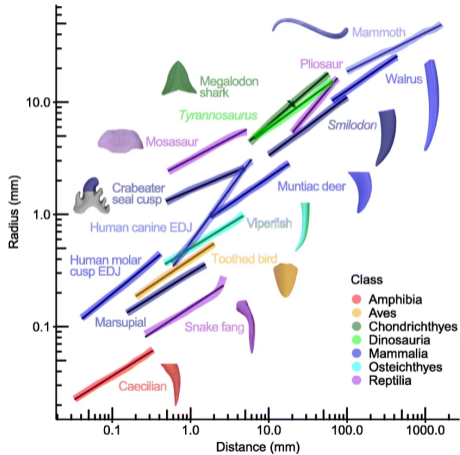
Low-Z vs. High-Z data



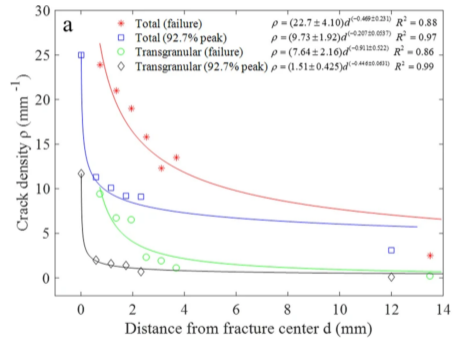
1. Update of the global H-mode confinement database and scaling
2. Regression analysis for scaling laws
 - Conventional techniques
 - Geodesic least squares regression (GLS)
3. The ITPA20 confinement scaling law
4. Conclusions

1. Update of the global H-mode confinement database and scaling
2. Regression analysis for scaling laws
 - Conventional techniques
 - Geodesic least squares regression (GLS)
3. The ITPA20 confinement scaling law
4. Conclusions

Ubiquity of power law models



A.R. Evans *et al.*, BMC Biology, 19, 58, 2021



F. Meng *et al.*, Scientific Reports, 9, 10705, 2019

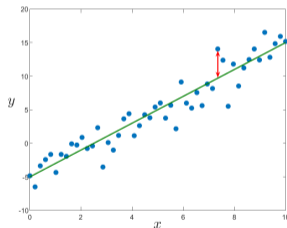
Least squares and maximum a posteriori estimation

- Multilinear regression model on logarithmic scale:

$$y = \alpha_0 + \alpha_1 x_1 + \alpha_2 x_2 + \dots + \alpha_p x_p + \epsilon$$

$$\epsilon \sim \mathcal{N}(0, \sigma^2), \sigma \text{ known}$$

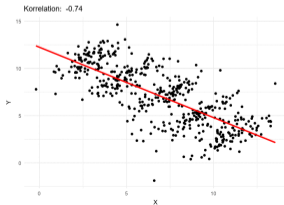
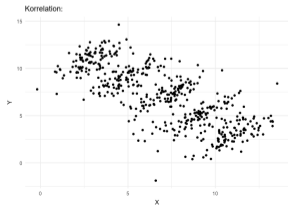
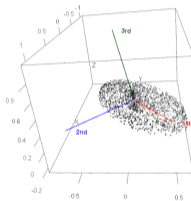
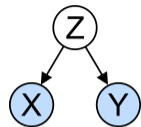
- Parameter estimation \rightarrow distance minimization:
expected \leftrightarrow measured
- Workhorse: ordinary least squares (OLS)
- Maximum likelihood (ML) / maximum *a posteriori* (MAP)



$$\frac{1}{\sqrt{2\pi}\sigma} \exp \left\{ -\frac{1}{2} \frac{\left[y - f(x, \theta) \right]^2}{\sigma^2} \right\}$$

Uncertainties in regression analysis

- Measurement uncertainty
- Model uncertainty:
 - Linear, power law, ...?
 - Missing variables
 - Confounding variables
- Multicollinearity: e.g. $I_p \propto B_t$
- Heterogeneity: multi-machine database
- Simpson's paradox:



Robust Bayesian regression

- Motivation:

- Outliers
- Measurement uncertainty
< total uncertainty
- Errors in all variables

$$\eta = \alpha_0 + \sum_{j=1}^p \alpha_j \zeta_j$$

$$y = \eta + \epsilon_y, \quad x_1 = \zeta_1 + \epsilon_{x_1}, \quad \dots$$

$$\epsilon_y \sim \mathcal{N}(0, \sigma_y^2), \quad \epsilon_{x_1} \sim \mathcal{N}(0, \sigma_{x_1}^2), \quad \dots$$

$$\sigma_{\text{mod}}^2 = \sigma_y^2 + \sum_{j=1}^p \alpha_j^2 \sigma_{x_j}^2$$

- Robust likelihood:

$$p(\{y_{i_k,k}\}, \{x_{i_k,j,k}\} | \{\alpha_0, \alpha_j\}, \{\gamma_k\})$$

$$= \prod_k \prod_{i_k} \frac{1}{\sqrt{2\pi\gamma_k^2\sigma_{\text{mod},i_k,k}^2}} \exp \left[-\frac{1}{2} \frac{(y_{i_k,k} - \eta_{i_k,k})^2}{\gamma_k^2 \sigma_{\text{mod},i_k,k}^2} \right]$$

1 for each device

1. Update of the global H-mode confinement database and scaling
2. Regression analysis for scaling laws
 - Conventional techniques
 - Geodesic least squares regression (GLS)
3. The ITPA20 confinement scaling law
4. Conclusions

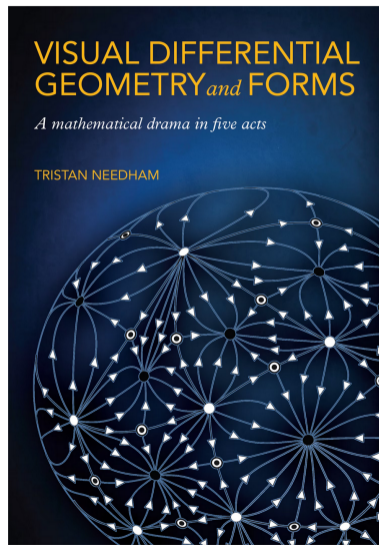
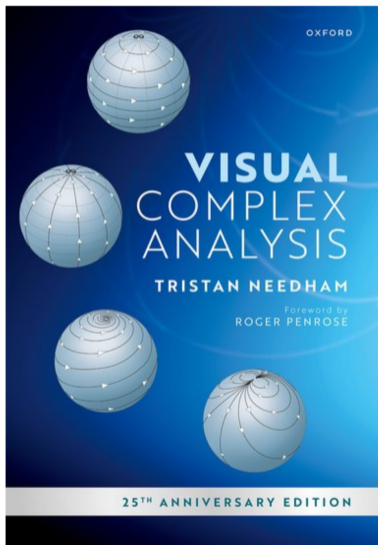
The power of simplicity

- Adoption in data-intensive communities
- Minimal parameter tuning
- Solid foundations

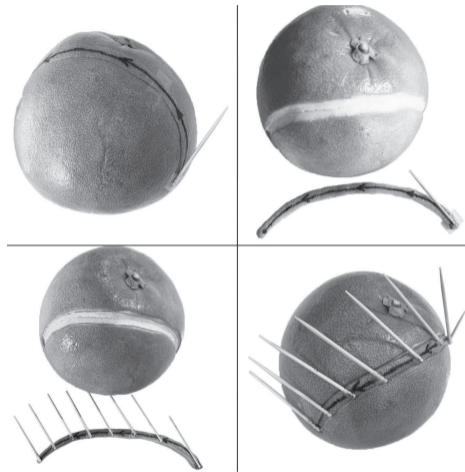
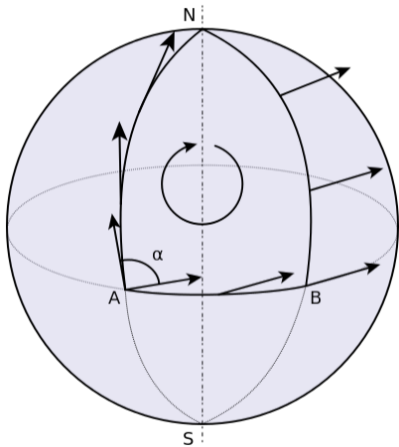


vs.

The power of visualization



Geodesics and parallel transport



T. Needham, 2021

The minimum distance approach

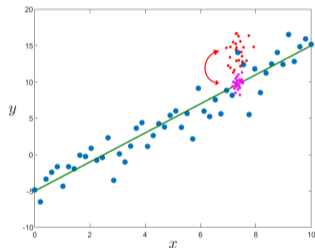
- *Minimum distance estimation* (Wolfowitz, 1952):

Which distribution does the model predict?

vs.

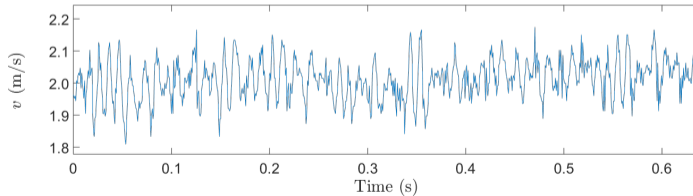
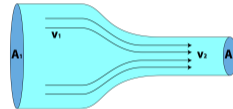
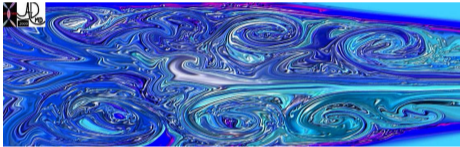
Which distribution do you observe?

- Gaussian case: different means *and* standard deviations
- Kullback-Leibler divergence, Hellinger divergence (Beran, 1977), ...
- Observed distribution: kernel density estimate



Number \rightarrow distribution

- Model observations by distributions
- More flexibility, more information



Information geometry

- Family of probability distributions \rightarrow differentiable manifold
- Parameters = coordinates
- Metric tensor: Fisher information matrix

Parametric probability model: $p(\mathbf{x}|\boldsymbol{\theta}) \implies$

$$g_{\mu\nu}(\boldsymbol{\theta}) = -\mathbb{E} \left[\frac{\partial^2}{\partial\theta^\mu \partial\theta^\nu} \ln p(\mathbf{x}|\boldsymbol{\theta}) \right], \quad \mu, \nu = 1, \dots, m$$

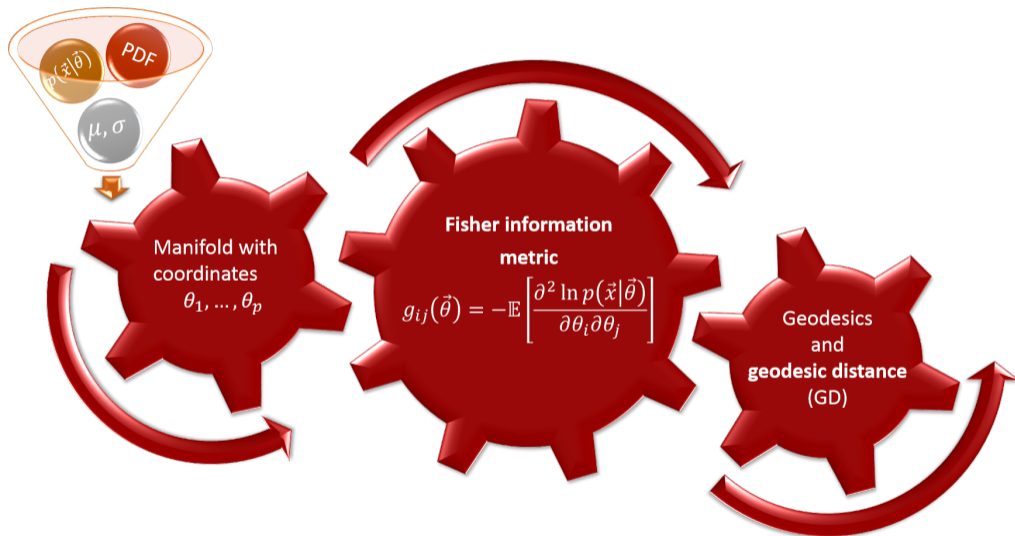
$\boldsymbol{\theta}$ = m -dimensional parameter vector

- Line element:

$$ds^2 = g_{\mu\nu} d\theta^\mu d\theta^\nu$$

- Minimum-length curve: *geodesic*
- *Rao geodesic distance* (GD)

Information geometry scheme



- Probability density function (PDF):

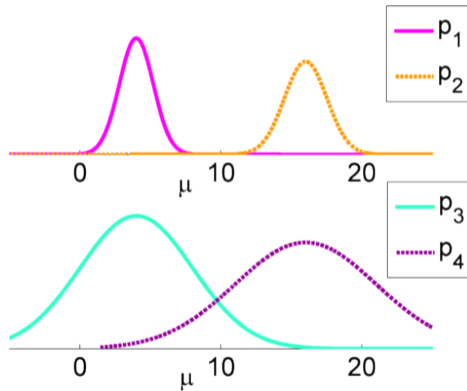
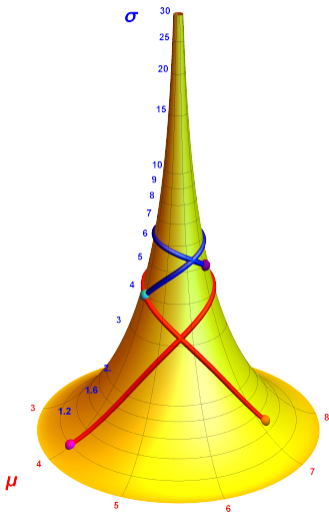
$$p(x|\mu, \sigma) = \frac{1}{\sqrt{2\pi}\sigma} \exp \left[-\frac{(x - \mu)^2}{2\sigma^2} \right]$$

- Line element:

$$ds^2 = \frac{d\mu^2}{\sigma^2} + 2\frac{d\sigma^2}{\sigma^2}$$

- Hyperbolic geometry: Poincaré half-plane model, pseudosphere, ...
- Analytic geodesic distance

Geodesic intuition: the pseudosphere



Geodesic least squares regression (GLS)

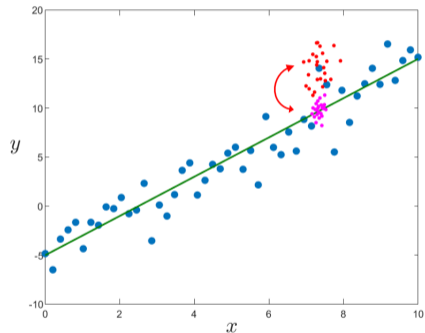
- Geodesic least squares: *GLS*

$$\prod_k \prod_{i_k} \frac{1}{\sqrt{2\pi\sigma_{\text{tot},i_k,k}^2}} \exp \left[-\frac{1}{2} \frac{(y_{i_k,k} - \eta_{i_k,k})^2}{\sigma_{\text{mod},i_k,k}^2} \right]$$



Rao geodesic distance (GD)

$$\frac{1}{\sqrt{2\pi} \sigma_{\text{obs}}} \exp \left[-\frac{1}{2} \frac{(y - y_i)^2}{\sigma_{\text{obs}}^2} \right]$$



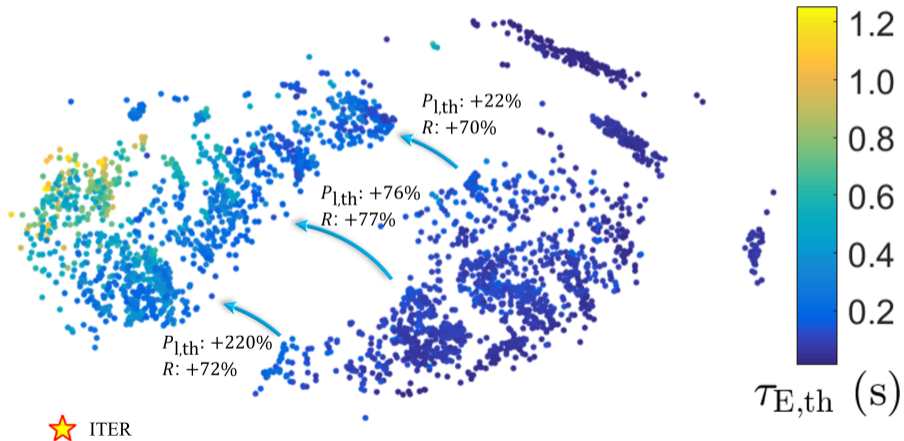
G. Verdoolaege *et al.*, Nucl. Fusion, **55**, 113019, 2015

G. Verdoolaege *et al.*, Entropy, **17**, 4602–4626, 2015

1. Update of the global H-mode confinement database and scaling
2. Regression analysis for scaling laws
 - Conventional techniques
 - Geodesic least squares regression (GLS)
3. The ITPA20 confinement scaling law
4. Conclusions

Database visualization by projection

- Multidimensional scaling
- Distance measure: Rao GD between Gaussian PDFs

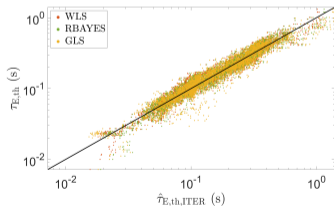


Multi-machine engineering scaling

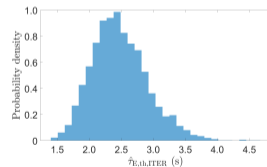
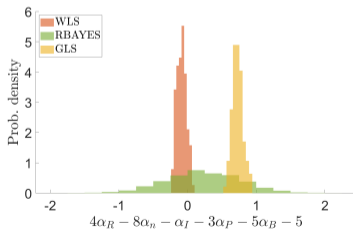
STD5-IL ELMy H-mode (error bars from Bayesian analysis)

Engineering scaling ITPA20-IL

$$\tau_{E,th} = (0.067 \pm 0.060) I_p^{1.29 \pm 0.17} B_t^{-0.13 \pm 0.17} \bar{n}_e^{0.15 \pm 0.10} P_{l,th}^{-0.644 \pm 0.060} R_{geo}^{1.19 \pm 0.29} \\ \times (1 + \delta)^{0.56 \pm 0.35} \kappa_a^{0.67 \pm 0.65} M_{eff}^{0.30 \pm 0.17}$$



$$RMSE = 0.17 \\ R^2 = 0.95$$

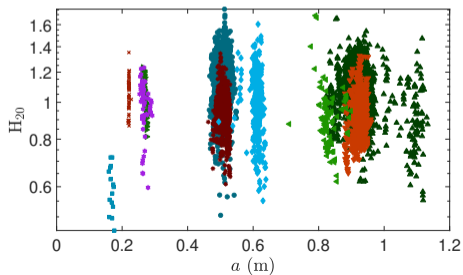
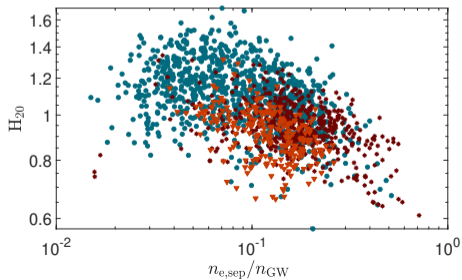
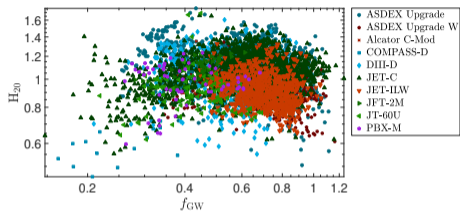
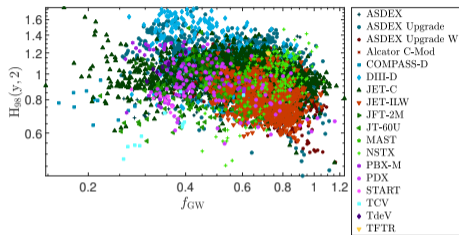


$$\hat{\tau}_{E,th,ITER} = \\ 2.90 \pm 0.46 \text{ s}$$

Quasi-neutral high- β Fokker-Planck with Landau collision operator + Ampère

Residuals

$$H_{20} \equiv \tau_{E,th} / \hat{\tau}_{E,th}$$



Multi-machine dimensionless scaling

- Transformation introduces large errors:

$$\alpha_D = A^{-1} \left(\frac{\alpha}{1 + \alpha_P} - a \right)$$

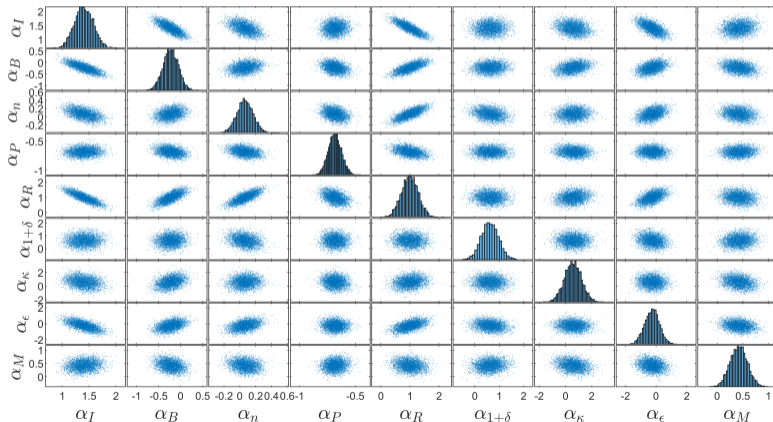
- Regression in dimensionless space

Dimensionless scaling ITPA20-IL-dim

$$\Omega_i \tau_{E,th} = (2.0 \pm 6.2 \times 10^{-6}) \rho_*^{-1.97 \pm 0.33} \beta_t^{0.12 \pm 0.21} \nu_*^{-0.425 \pm 0.062} q_{cyl}^{-1.03 \pm 0.42} \\ \times (1 + \delta)^{0.14 \pm 0.63} \kappa_a^{1.90 \pm 0.81} \epsilon^{-0.26 \pm 0.62} M_{eff}^{0.61 \pm 0.37}$$

Error analysis

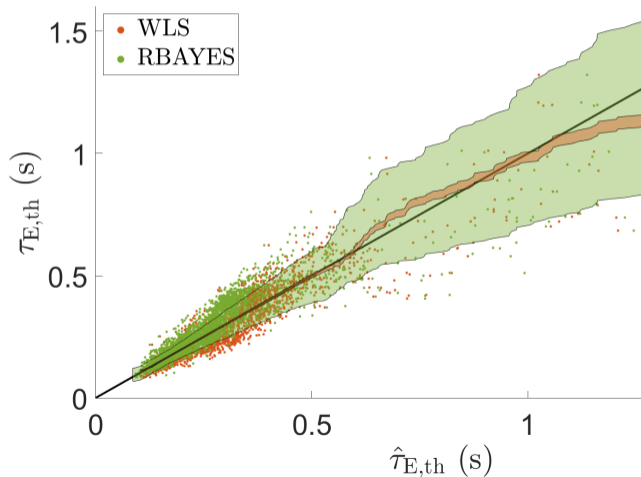
- Sensitivity analysis under multicollinearity: $\sim 10\times$ larger error bars
- Observed uncertainty \gg modeled uncertainty



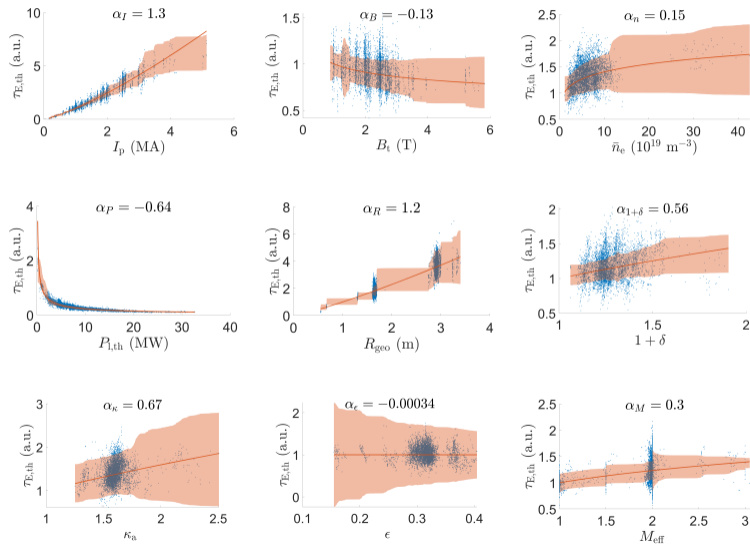
MCMC sampler
with 4 chains

Uncertainty calibration

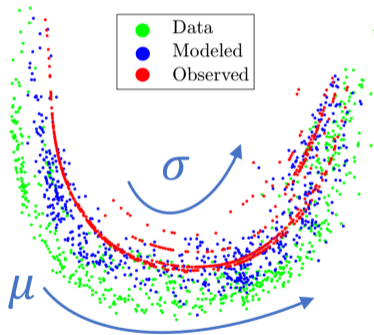
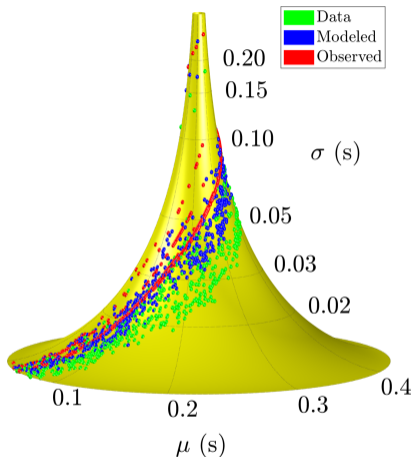
- Predictions for JET
- Confidence bands (smoothed):



Confinement trends



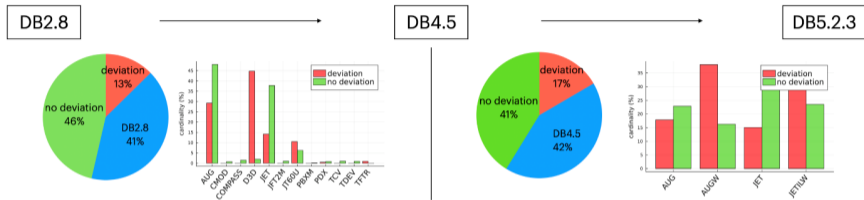
Visualization on pseudosphere and projection



	AUG	AUG-W	Alcator C-Mod	COMPASS-D	DIII-D	JET-C	JET-ILW	JFT-2M	JT-60U	PBX-M
γ_k	0.96	0.79	0.51	3.8	0.85	1.0	0.89	0.69	1.1	0.85
$\sigma_{\text{obs},k}/\sigma_{\text{mod},k}$	1.2	1.1	1.2	2.0	1.2	1.2	1.2	1.1	1.2	2.0

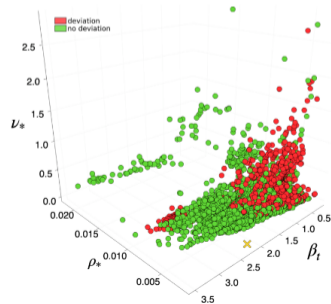
Origin of reduced size scaling

- Clustering 'deviation' vs. 'no-deviation' set:



- Scaling for 'no deviation' set:

$$\tau_{E,th} = 0.07 I_p^{0.87} B_t^{0.20} \bar{n}_e^{0.38} P_{l,th}^{-0.74} R_{geo}^{2.0} \times \kappa_a^{0.41} \epsilon^{0.59} M_{eff}^{0.24}$$



1. Update of the global H-mode confinement database and scaling
2. Regression analysis for scaling laws
 - Conventional techniques
 - Geodesic least squares regression (GLS)
3. The ITPA20 confinement scaling law
4. Conclusions

Conclusions

- Revision of global confinement scaling with realistic error estimates
- Significant uncertainty on parameter estimates, exacerbated by multicollinearity
- ITER predictions ca. 20 – 25% lower
- Size dependence lowered by relatively small subset at high ν_*
- Advantages of geodesic least squares regression:
 - Simple, fast and robust
 - Visual interpretation
- Wider applicability to parameter estimation, model validation, etc.

Number of database entries

Device	DB2.8		DB5.2.3		
	ELMy H	STD ₅		STD ₅ ITER-like	
		All H	ELMy H	ELMy H	ELM-free H
ASDEX	431	575	431	0	0
AUG	102	1385	1377	1370	8
AUG-W	0	767	767	767	0
Alcator C-Mod	37	82	45	45	37
COMPASS-D	0	21	16	16	5
DIII-D	270	502	388	383	114
JET-C	246	2211	1762	1606	426
JET-ILW	0	866	866	855	0
JFT-2M	59	348	69	59	197
JT-60U	9	100	100	100	0
MAST	0	43	43	0	0
NSTX	0	230	185	0	0
PBX-M	59	214	59	59	155
PDX	97	119	97	0	0
START	0	8	8	0	0
T-10	0	4	0	0	0
TCV	0	17	11	0	0
TdeV	0	7	7	0	0
TEXTOR	0	0	0	0	0
TFTR	0	2	2	0	0
TUMAN-3M	0	36	0	0	0
Total	1310	7537	6233	5260	942

- 14 153 points from 19 tokamaks
- ‘Standard set’ **STD5** → 7 537 points from 18 devices:
 - Quasi steady-state H-modes, no pellets, no ITBs
 - Limited P_{rad} , W_{fast} , l_i ; minimum q_{95}
 - Limited $T_e \neq T_i$
- ‘ITER-like’ **STD5-IL** → 6 202 points from 8 devices:
 - $q_{95} > 2.8$
 - $1.3 < \kappa < 2.2$
 - $\epsilon = a/R_{\text{geo}} < 0.5$
 - $Z_{\text{eff}} < 5$
- High-Z: Alcator C-Mod, AUG-W, JET-ILW